

DESIGN OF MULTICOMPONENT ALLOYS ON THE BASE OF Al-Ca EUTECTICS WITHOUT REQUIREMENT FOR QUENCHING

*N. A. Belov¹, E. A. Naumova¹, T. K. Akopyan^{1,2}, and V. V. Doroshenko¹

¹*National University of Science and Technology MISiS, Moscow, Russia*
(*Corresponding author: nikolay-belov@yandex.ru)

²*Baikov Institute of Metallurgy and Materials Science, Moscow, Russia*

ABSTRACT

A qualitative and quantitative analysis of the new Al-Ca-Mn-Fe phase diagram in the region of the aluminium corner is carried out using both thermodynamic calculations and experimental methods. Using the obtained data, the principal possibility of creating both cast and wrought sparingly alloyed aluminium alloys with calcium, manganese, scandium and zirconium at allowable iron contents of up to 0.4% that do not require solution treatment and quenching is justified. At the selected concentrations, the entire amount of manganese (1%) is practically included in the aluminium matrix, while calcium (~2%) and iron are in the multiphase eutectic, which has a fine structure. The joint introduction of 0.25% Zr and 0.1% Sc into the alloy leads to precipitation hardening due to the formation of the $L1_2$ -Al₃(Zr,Sc) phase during annealing. Based on the experimental data for the model multicomponent Al₂CaMnFeZrSc alloy, it is shown that such alloys can combine high mechanical properties and good manufacturability during both casting and metal forming. This is due to the combination of a narrow temperature range of solidification with a fine eutectic structure.

KEYWORDS

Aluminium-calcium eutectic, Hardening, Nanoparticles, Phase composition

INTRODUCTION

Hardening in branded aluminium alloys (both cast and wrought) is generally achieved by heat treatment of the T6 type, including quenching and artificial aging (Zolotorevskiy, 2007; Kaufman, 2004; Mondolfo, 1976). Heat treatment significantly increases the cost of the final products. Therefore, industrial companies are interested in developing alloys that can be hardened to the desired level without quenching. To solve this problem, alloys with scandium are the most suitable (Toropova, 1998; Røyset, 2005). This element (usually in an amount of ~0.3%) is one of the most effective hardeners in aluminium alloys, due to the formation of Al_3Sc ($L1_2$) phase secondary precipitates, the size of which is less than 10 nm (Knipling, 2010; Fuller, 2005). These nanoparticles are formed during the annealing via decomposition of the supersaturated aluminium solid solution (hereinafter referred to as (Al)). This feature allows us to significantly increase the strength of aluminium alloys by simple annealing (at ~300°C), i.e., without heat treatment, including quenching. However, scandium is a very expensive metal, so its use as an additive is severely limited. The most effective method is the introduction of scandium together with zirconium (Lefebvre, 2009; Booth-Morrison, 2012). The optimal combination is the introduction of ~0.1% Sc together with 0.20–0.25% Zr, which, according to (Belov, 2006), gives approximately the same strengthening effect as the introduction of 0.3% Sc.

Among wrought alloys, the most suitable for the realisation of the maximum hardening effect due to $L1_2$ nanoparticles are alloys of the Al-Mg-Mn system (3xxx and 5xxx series) (Mondolfo, 1976). However, due to their low casting properties, such alloys can only be used very narrowly to produce complex castings. Alternatively, in Al-Si alloys, which are the main group (3xx series) of casting aluminium alloys, the introduction of scandium and zirconium is useless, since it does not lead to appreciable hardening (Toropova, 1998; Belov, 2015). Among other eutectic systems, in which the introduction of Zr and Sc can achieve hardening by the heat treatment of the T5 type, it should be noted that the alloys of Al-Ni system make it possible to achieve a successful combination of mechanical and cast properties (Belov, 2004). However, nickel leads to a decrease in the overall corrosion resistance, as well as an increase in alloy density. Therefore, it is advisable to consider other alloying systems, in particular, those based on the aluminium-calcium eutectic. In the work (Belov, 2015), using the model Al-7.6% Ca-0.3% Sc alloy, the principal possibility of creating such alloys is substantiated. To create alloys sparingly alloyed with scandium (no more than 0.1%) and with a sufficiently high range of operational and technological properties, an analysis of more complex alloying systems, in particular, additionally containing manganese, zirconium and iron, is required.

Based on the above and taking into account the scarcity of information on aluminium alloys with calcium addition (especially multicomponent), the main objectives of this work are identified as:

- 1) Study the phase diagram of the Al-Ca-Mn-Fe-Zr-Sc system using both thermodynamic calculations and experimental methods.
- 2) Justify the composition of the multicomponent model aluminium alloy for both wrought and cast products without the requirement for solution treatment and quenching.
- 3) Study the effect of precipitation hardening due to formation of the $L1_2$ - Al_3 (Zr,Sc) phase nanoparticles of the model alloys.
- 4) Study of the basis set of mechanical and technological properties of the model alloy.

CALCULATION OF PHASE DIAGRAM

The selection of this alloying system as the basis for the development of new casting alloys, which can be hardened without quenching, is determined by the following considerations. Calcium is the main eutectic-forming element, and largely determines the castability of the alloy (Belov, 2015). In addition, calcium has a positive effect on corrosion resistance and reduces the density of the alloy (Mondolfo, 1976). Manganese may be dissolved in the as-cast (Al) to increase the strength properties. A significant effect is achieved with a Mn content of 1% or more (Zolotorevskiy, 2007; Kaufman, 2004; Mondolfo, 1976). Iron is an unavoidable impurity in primary aluminium and is practically insoluble in (Al). The mechanical properties (particularly ductility) of castings and wrought products largely depend on the morphology of

Fe-containing phases (Zolotarevskiy, 2007; Moustafa, 2009; Ji, 2013; Basak, 2016). Zirconium and scandium, as noted above, are necessary for hardening due to the formation of $L1_2$ nanoparticles during the heterogenisation annealing of castings and ingots (Toropova, 1998; Røyset, 2005; Belov, 2006).

Based on the available information (Mondolfo, 1976; Belov, 2005), Al_4Ca , Al_9CaMn_3 , Al_3Fe , $Al_6(Fe,Mn)$, Al_3Zr and Al_3Sc can be in equilibrium with (Al) in the alloys of the considered system. According to (Belov, 2017), iron and calcium form a ternary compound with aluminium, whose composition corresponds to the formula $Al_{10}CaFe_2$. Zirconium and scandium do not form phases with the other elements of the system (except aluminium). Therefore, it is sufficient to analyse the quaternary Al-Ca-Mn-Fe system to select the optimum concentrations of calcium, manganese and iron.

Analysis of the phase composition of the six-component alloys was carried out using calculations in the Thermo-Calc program (<http://www.thermocalc.com>, 2017). Since there are no ternary compounds Al_9CaMn_3 and $Al_{10}CaFe_2$ in the thermodynamic database (TTAL5), the results of the calculation were critically evaluated taking into account this incompleteness.

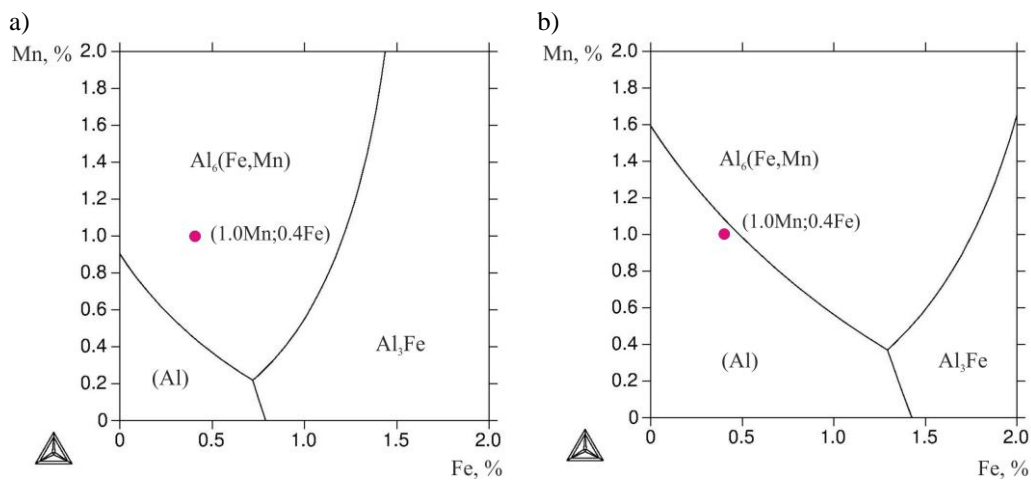


Figure 1. Liquidus projection of Al-Ca-Mn-Fe system at a) 6 wt.%Ca and b) 2 wt.%Ca

Initially, assuming that the presence of primary intermetallic crystals is certainly undesirable, the region of primary crystallisation of (Al) was estimated. It was also assumed that additional alloying should reduce the eutectic concentration of calcium, which in the binary system is 7.4–7.6% (Mondolfo, 1976; Belov, 2015; Kevorkov, 2001). To estimate the maximum allowable concentrations of iron and manganese, the boundaries of the liquidus surface of the Al-Ca-Mn-Fe system with different calcium contents were calculated. As can be seen from Figure 1a, at 6% Ca, the total concentration of Fe and Mn, at which the primary crystals of Fe and Mn-containing phases are not formed, does not exceed 1%. With a decrease in the calcium content, the region of the (Al) primary crystallisation is expanded. At 2% Ca, the alloy with 1% Mn admits at least 0.4% Fe (Figure 1b). Therefore, the composition of Al-2% Ca-1% Mn-0.4% Fe was selected as the base. According to the analysis of the Al-Ca-Fe-Mn system, during solidification of this alloy, after formation of a small amount of the (Al) primary crystals, the eutectic reaction $L \rightarrow (Al) + Al_6(Fe, Mn)$ should occur. Solidification of this alloy should be completed via the four-phase eutectic reaction $L \rightarrow (Al) + Al_6(Fe, Mn) + Al_4Ca$, which although is monovariant, has a temperature range that is very small (less than $1^\circ C$). Since the total temperature range of solidification of the Al-2% Ca-1% Mn-0.4% Fe alloy is relatively small ($\sim 35^\circ C$), we would expect good castability, as confirmed experimentally (see below). At higher contents of iron there is a danger of the occurrence of $Al_6(Fe,Mn)$ phase primary crystals, as well as an increase in the liquidus temperature, which is evident from the Scheil-Gulliver simulation shown in Figure 2.

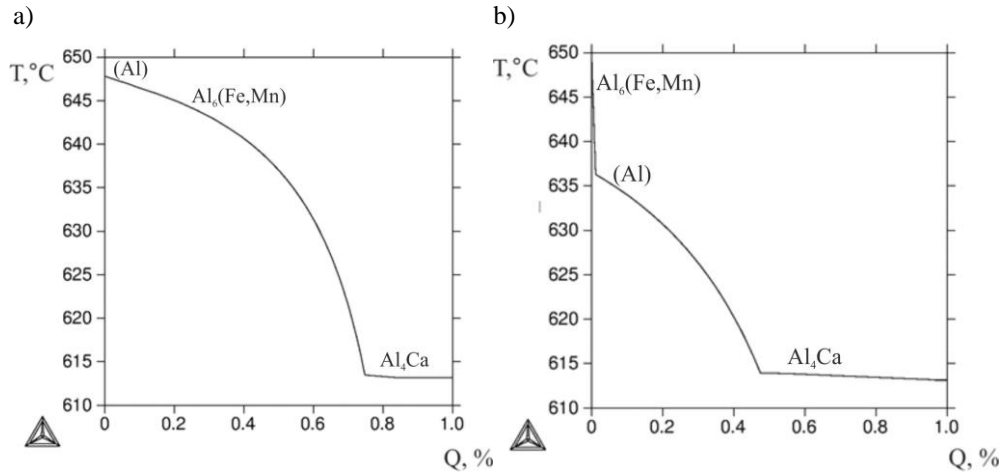


Figure 2. Calculated Q-T curves (Sheil-Gulliver simulation) for the alloys a) Al₂Ca1Mn0.4Fe and b) Al₆Ca1Mn0.4Fe

The influence of zirconium and scandium on the boundaries of the appearance of primary crystals of intermetallic phases in the selected alloy is reflected in Figure 3a, from which we can see that at 0.1% Sc and 0.25% Zr, the Al₃Zr aluminide should initially form. However, it is known that at the cooling rates typical for the casting in metal moulds (5–20°C/s), the concentration boundary is shifted toward higher zirconium concentrations (Vlach, 2012), as shown by the dashed lines. Therefore, it was assumed that the total amount of Zr and Sc should enter into the (Al) composition and consequently have no influence on the phase composition of the Al-2% Ca-1% Mn-0.4% Fe alloy, as considered above. However, when these additions are present, the casting temperature should be higher than in the base alloy, which is associated with an increase in the liquidus temperature from 645 to 760°C. This follows from the vertical section shown in Figure 3b.

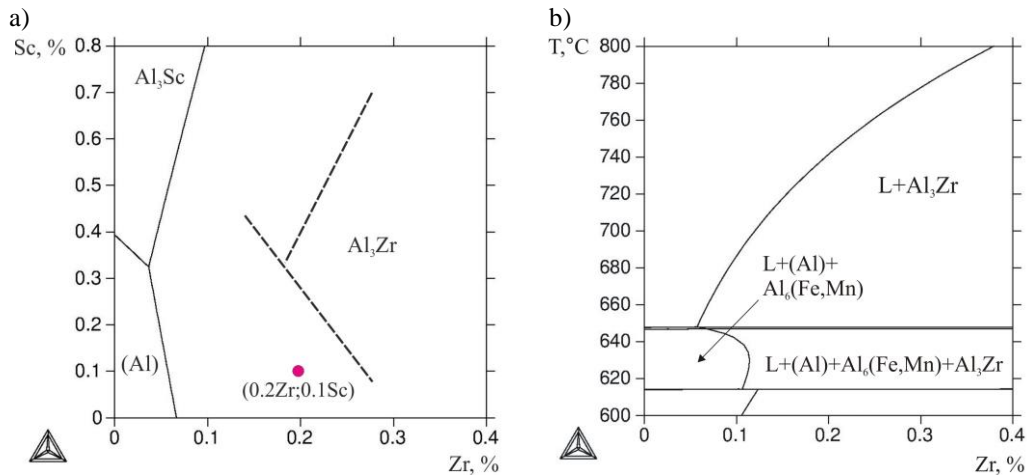


Figure 3. a) Liquidus projection and vertical section of Al-Ca-Mn-Fe-Zr-Sc system at 2%Ca, 1%Mn, and 0.4%Fe: dotted lines – shift after unequilibrium solidification, b) at 0.1%Sc

If we proceed from the fact that in the as-cast state the entire amount of manganese, zirconium and scandium is included in the (Al) (small solubilities of calcium and iron can be neglected), it becomes possible to calculate the amount of secondary precipitates at the appropriate temperature. The results of this calculation at 400°C are given in Table 1. It was assumed that annealing at this temperature would allow us to obtain the maximum hardening (Belov, 2006). Since this hardening is associated with the formation of

L₁₂ phase nanoparticles, the stable phase Al₃Zr (D0₂₃) was excluded from the calculation. It follows from these results that the total volume fraction of the secondary precipitates should be more than 3 vol.%, which is comparable with thermally hardenable alloys of 356/357 type and after the T6 heat treatment regime (Abdulwahab, 2011; Liao, 2013).

Table 1. Calculated phase composition of alloy Al–1%Mn–0.25%Zr–0.1%Sc at 400 °C

Phase	Q _M , wt.%	Q _V , vol.%	Concentration in phase, wt.%			
			Mn	Zr	Sc	Al
Al ₆ Mn	3.55	2.84	25.34	–	–	74.66
L ₁₂ - Al ₃ (Zr,Sc)	0.61	0.54	–	31.15	14.71	54.13
(Al)	95.84	96.62	0.11	0.06	0.01	98.82

EXPERIMENTAL METHODS

The main subject of the experimental study is the alloy of the selected composition (hereinafter Al₂CaMnFeZrSc). The melting was carried out in an electric resistance furnace in a graphite-chased crucible based on high purity aluminium (99.99%). Calcium, manganese, iron, zirconium and scandium were introduced into the aluminium melt in the form of binary master alloys (Al-15%Ca, Al-10%Mn, Al-10%Fe, Al-15%Zr and Al-2%Sc, respectively). The casting was carried out in a graphite mould at a temperature of ~780°C to obtain flat ingots with dimensions of 15×30×180 mm (the cooling rate during solidification was ~10 K/s). Samples were extracted from the obtained castings to study the structure and properties. The chemical composition of the experimental alloy according to spectral analysis (Oxford Instruments) is given in Table 2, from which it can be seen that the actual composition is very close to the given one.

Table 2. Chemical composition of experimental alloy Al₂CaMnFeZrSc

Concentration, wt %					
Ca	Mn	Fe	Zr	Sc	Al
2.03±0.11	1.01±0.04	0.47±0.04	0.22±0.08	0.13±0.03	96.14±0.11

The estimation of casting properties was carried out using various probes for hot tearing (Zolotorevskiy, 2007), as well as by producing shaped castings into metal moulds. The deformation ability (both hot and cold) was evaluated by obtaining various deformed semi-finished products.

The heat treatment of the castings was carried out in muffle electric furnaces with a temperature accuracy of ~3 K. Multi-step annealing modes in the temperature range from 200 to 600°C with a step of 50°C and a 3-h exposure at each step were used. After each annealing step, the samples were cooled in air. The stepwise mode allows us to carry out all studies of the influence of heating temperatures on one sample. This method was both informative and economical for the Al alloys, which hardened due to the nanoparticles of the L₁₂ phase (Belov, 2006).

The microstructure was examined by means of optical microscopy (OM, Olympus GX51), transmission electron microscopy (TEM, JEM–2100), scanning electron microscopy (SEM, TESCAN VEGA 3) and by electron microprobe analysis (EMPA, OXFORD AZtec). Polished samples were used for the studies. Mechanical polishing was used, as well as electrolytic polishing, which was carried out at a voltage of 12 V in an electrolyte containing six parts C₂H₅OH, one part HClO₄ and one part glycerine. The initial analysis of the microstructure of the samples was carried out using OM and detailed metallographic studies were performed using SEM. The thin foils for TEM were prepared by ion thinning with a PIPS (Precision Ion Polishing System, Gatan) machine and studied at 160 kV.

Differential scanning calorimetry (DSC) with a heating and cooling rate of 10 K/min was performed using a high-temperature Setaram Setsys Evolution on specimens with a mass of ~80 mg. The experiment was carried out in a dynamic Ar atmosphere with a flow rate of 50 ml/min. A temperature accuracy of ±0.5°C was obtained.

The Brinell hardness was determined in a INNOVATEST (series NEMESIS 9000) hardness testing machine with a ball diameter of 2.5 mm, a load of 612.9 N and a dwell time of 30 s. The specific electrical conductivity (Ω) was measured by eddy-current testing using a VE-26NP device with high purity Al (99.99%) as an additional standard. A Zwick Z250 machine was used for tensile tests (the velocity of loading was 10 mm/min). The density was determined using the Archimedes method on laboratory electronic scales (HR-202i). Tests for intergranular corrosion were carried out in a 3% solution of NaCl + 1% HCl solution at a temperature of 20°C for 24 h.

RESULTS AND DISCUSSION

Structure, Phase Composition and Hardening of Al₂CaMnFeZrSc Alloy

The microstructure of the Al₂CaMnFeZrSc alloy looks reasonably uniform (Figure 4a). The main structural components are both primary crystals of (Al) and eutectic colonies with a fine structure. The eutectic colonies are vein-shaped and located along the boundaries of (Al) dendritic cells, whose average size is ~50 μm (Figure 4a). Calcium is concentrated in the eutectic (Figure 4b). On the general background of the eutectic, separate skeletal inclusions with an increased content of manganese (Figure 4c) and iron (Figure 4d) are found. This allows us to identify them as the Al₆(Fe, Mn) phase, which formed in the process of the $L \rightarrow (Al) + Al_6(Fe, Mn)$ eutectic reaction (as follows from Figures 2 and 3b). The eutectic colonies probably consist of three phases ((Al), Al₆(Fe, Mn) and Al₄Ca), or with a larger number of phases (including the possible formation of ternary Ca-containing compounds; see Table 1). Manganese, as can be seen from Figure 4c, enters not only in the eutectic composition, but also in the primary crystals (Al).

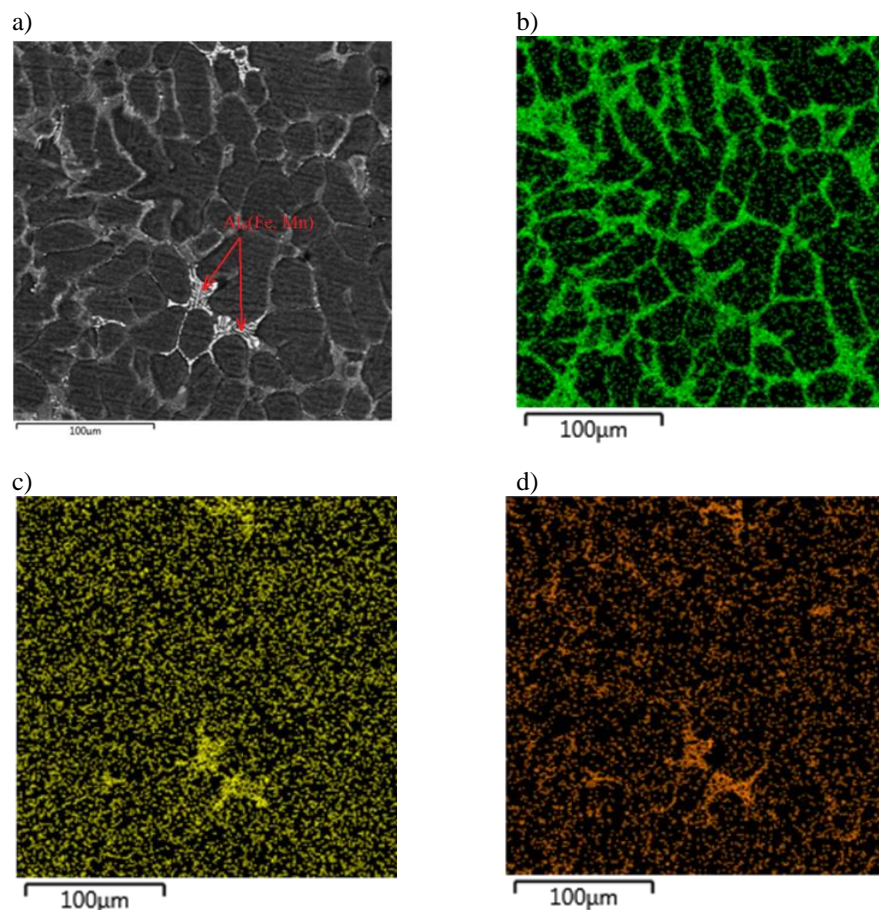


Figure 4. BSE image (a) and EMPA elemental mapping of (a) Ca, (b) Mn, (c) Fe for the as-cast alloy Al₂CaMnFeZrSc

Quantitative analysis of the chemical composition of (Al) shows (Table 3) that the manganese concentration is 0.95%, i.e., 95% of its total amount in the alloy (Table 2). The concentration of scandium in (Al) is also close to its concentration in the alloy. The higher measured zirconium concentration is probably due to the fact that its distribution coefficient is greater than 1 and as a result it is predominantly concentrated in the centres of the dendritic cells (Zolotarevskiy, 2007), into which the electron probe was focused. In addition, a sufficiently large typical range of values is characteristic for zirconium, which can be explained by its increased segregation. The contents of iron and calcium in (Al), as expected, are negligible.

According to the DSC data, the liquidus and solidus temperatures of the Al₂CaMnFeZrSc alloy are 650 and 613°C, respectively (Figure 5a), which are close to the calculation results (see Figure 2a), if the additions of zirconium and scandium are not taken into account. Thus, the total temperature range of solidification is 37°C, which is less than for the 356 alloy (47°C). Taking into account the non-equilibrium solidification, the difference is even greater (40 versus 58°C), since the presence of magnesium in the 356 alloy leads to the formation of a non-equilibrium eutectic at 555°C (Zolotarevskiy, 2007).

The presence of a given amount of Zr and Sc in (Al) in the as-cast state suggests the possibility of precipitation hardening due to (Al) decomposition during annealing. The decomposition process of (Al) was investigated using the measurements of hardness and specific electrical resistivity, as well as TEM. As can be seen from Figure 5b, at 200°C, hardening is absent, whereas at 250°C, it is already noticeable. The highest hardness values are achieved at 300–450°C. At the same time, in the reference binary alloy Al-0.3% Sc, annealing at temperatures above 300°C leads to softening, which is very significant at 450°C. During decomposition of (Al) in the Al₂CaMnFeZrSc alloy, the electrical conductivity also increases as hardness, but the maximum shifts to 500°C. At the higher temperatures, the specific conductivity is decreased, which is explained by an increase in the concentrations of Mn, Zr and Sc in (Al). Thus, the combined introduction of 0.1% Sc and 0.25% Zr provides not only a hardening effect, which is comparable to hardening in the case of 0.3% Sc, but also increases the softening temperature (i.e., thermal stability).

TEM makes it possible to detect the decomposition products of (Al), as well as more reliably detecting the size and morphology of particles within the eutectic. As can be seen from Figure 6a, the aluminium-calcium eutectic shows evidence of a multiphase structure. Simultaneously, the aluminide particles have a compact morphology, and their thickness is ~100 nm. Heating up to 400°C does not affect the morphology of these particles. Taking into account the analysis of (Al) composition in the as-cast state (Table 3), only 0.05% of Mn can enter the phases of eutectic origin. Based on the fact that virtually all amounts of calcium and iron are in the eutectic phases, a composition of Al-2% Ca-0.4% Fe-0.05% Mn was chosen for the calculation. The calculation has showed that except (Al), the eutectic contains the following phases: Al₄Ca, Al₆(Fe,Mn) and Al₃Fe in amounts of 7.39, 0.35 and 0.89 wt.%, respectively. Taking into account that the TTA15 base does not contain ternary Ca-containing compounds (with iron and manganese), the presence of the Al₁₀CaFe₂ phase instead of Al₃Fe is most likely.

Table 3. Chemical composition of aluminium solid solution in as-cast alloy Al₂CaMnFeZrSc

Concentration, wt.%*					
Ca	Mn	Fe	Zr	Sc	Al
0.02±0.02	0.95±0.09	0.03±0.04	0.43±0.15	0.07±0.02	98.50±0.02

*centers of dendrite arms

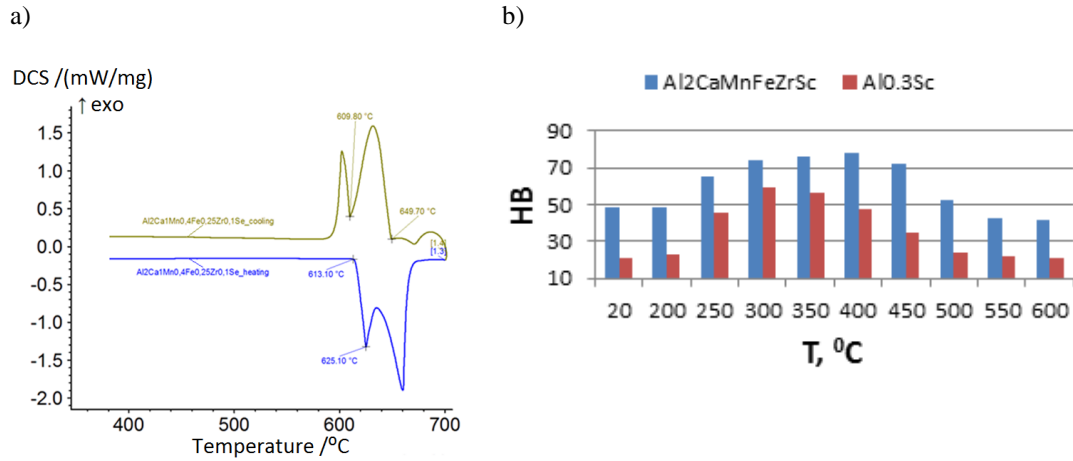


Figure 5. DCS curve (a) and hardening effect (b) for alloy Al₂CaMnFeZrSc

The TEM structures, shown in Figure 6, confirm the presence of secondary precipitates containing zirconium and scandium, in the state of maximum hardening. In particular, the light-field images allow for the detection of contrasts of the "coffee beans" type from these particles, and microdiffraction has superstructural reflexes, which are characteristic of the L₁₂ phase (Figure 6b). The darkfield images obtained from these reflections show the presence of uniformly located particles of the Al₃(Zr, Sc)-L₁₂ phase, with a size of less than 10 nm (Figure 5b). The presence of secondary precipitates of the Al₆Mn phase with an orthorhombic lattice. The size of these precipitates is ~200 nm (Figure 6c), which is quite typical (Belov, 2006). In general, the experimental alloy structure is reasonably suitable to expect a sufficiently high complex of mechanical and physical properties.

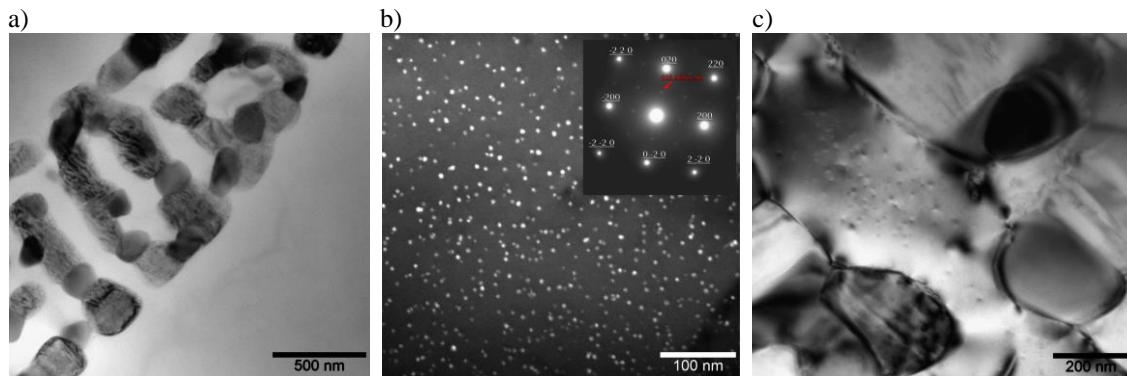


Figure 6. TEM structure of alloy Al₂CaMnFeZrSc after annealing T400 (see in Table 4), TEM: a,c) bright field, b) dark field and diffraction pattern for phase Al₃(Zr,Sc)-L₁₂

Manufacturability and Mechanical Properties of Al₂CaMnFeZrSc Alloy

Based on the known empirical laws, the narrow solidification range suggests excellent casting properties (Zolotarevskiy, 2007). The experimental results confirm this suggestion. In particular, according to the "pencil" (Toropova, 1998) and "harp" (Zolotarevskiy, 2007) probes, these alloys are not inferior to standard Al-Si eutectic alloys. As an example, a shaped casting of the Al₂CaMnFeZrSc alloy is shown in Figure 7a, which was obtained in an industrial mould, designed for the 356 alloy. The viewed alloy also showed good manufacturability during ejection die casting. The injection die produced (from one pouring) four flat tensile samples 15 mm wide with four different thicknesses of 1.9, 2.8, 5.1 and 6.5 mm. Visual inspection of cast samples did not reveal cracks, pores and other castings defects. The high stability of the

mechanical properties of the alloy Al₂CaMnFeZrSc given in Table 4 should be noted. In particular, the scatter of the UTS values does not exceed 10 MPa.

Since annealing enables us to achieve the precipitation hardening due to formation of the L1₂ precipitates (Figs. 6b), the mechanical properties of the castings can be increased. As can be seen from Table 4, the mechanical properties of the castings, which were obtained in a graphite mould and then annealed at 300°C for 3 h + 400°C for 3 h, are comparable to the 356.0 alloy, heat-treated according to the T6 regime.

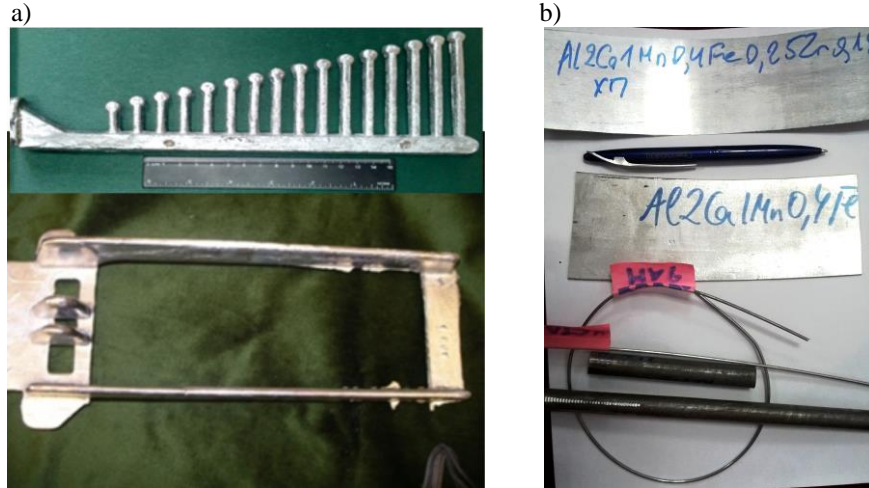


Figure 7. a) Castings and b) wrought products from alloy Al₂CaMnFeZrSc

Table 4. Mechanical properties of alloy Al₂CaMnFeZrSc

Kind of alloy	Heat treatment	HV, MPa	UTS, MPa	YS, MPa	El, %
Die casting	As cast	500	156 ± 17	111 ± 7	2.2 ± 0.7
Permanent (graphite) mold casting	Annealed (300°C, 3 h +400°C, 3 h)	780	247 ± 10	156 ± 5	5.3 ± 0.4
Hot rolled sheet (2.3mm)	After rolling	810	288 ± 3	257 ± 5	1.0 ± 0.2
	Annealed (350°C, 3 h)	740	254 ± 3	205 ± 2	3.0 ± 0.5
Wire	After drawing	–	325 ± 3	284 ± 4	2.5 ± 0.4

The deformability of the experimental alloy was evaluated by obtaining various semi-finished products: sheets, bars and wires (Figure 7b). In particular, the possibility of obtaining high-quality sheets (2.3 mm thick) from cast (non-heat treated) ingots (15×30×100 mm in size) at a temperature of 350 °C is shown. The strength properties of the obtained in hot-rolled sheets are significantly higher than for the castings (see Table 4). Subsequent annealing at 350°C improves elongation three times with some reduction of strength.

The Al₂CaMnFeZrSc alloy also demonstrated good manufacturability during cold rolling and drawing (see Figure 7b). The resulting sheets (0.5 mm thick) and wire (2 mm in diameter) had no visible defects. As expected, the cold deformation can achieve greater strength compared to hot deformation. In particular, in the wire, the UTS value is more than 300 MPa with satisfactory ductility (see Table 4).

Thus, the possibility of creating both cast and wrought sparingly alloyed aluminium alloys with calcium (~2 wt.%) and scandium (~0.1 wt.%), which do not require quenching, was justified in this work. Despite the small amount of the eutectic, such alloys can have a high castability due to the narrow

temperature range of solidification. Alternatively, in the case of the multicomponent Al₂CaMnFeZrSc alloy, the good manufacturability of non-homogenised ingots during the metal forming is shown. The high deformability of the alloy is due to the fine structure of the aluminium-calcium eutectic.

CONCLUSIONS

1. Analysis of the phase composition of Al-Ca-Mn-Fe system aluminium alloys using calculation methods has allowed for substantiation of the optimal concentrations of calcium (2%) and manganese (1%) at an allowable iron content of up to 0.4% inclusive.
2. At the selected concentrations, the entire amount of manganese is practically included in the aluminium matrix, while calcium and iron are in the multiphase eutectic, which has a fine structure. With an increase in the calcium content (more than 2%), the formation of the primary Al₆(Fe,Mn) phase crystals should be expected.
3. It is shown that the joint introduction of 0.25% Zr and 0.1% Sc into the alloy of the selected composition allows to realize the effect of precipitation hardening due to the L1₂-Al₃(Zr,Sc) phase nanoparticles, without quenching. This hardening is maintained up to 450°C. Softening occurs at higher temperatures, which is associated with the coarsening of these particles.
4. For the example of the multicomponent alloy Al₂CaMnFeZrSc, the possibility of creating casting and wrought alloys based on aluminium-calcium eutectics additionally alloyed with manganese, zirconium and scandium is substantiated. Such alloys can combine high mechanical properties and good manufacturability during both casting and metal forming.

ACKNOWLEDGMENTS

The work was supported by the Russian Science Foundation grant 14-19-00632P.

REFERENCES

- Abdulwahab, M., Madugu, I.A., Yaro, S.A., Hassan, S.B., & Popoola, A.P.I. (2011). Effects of multiple-step thermal ageing treatment on the hardness characteristics of A356.0-type Al-Si-Mg alloy. *Materials and Design*, 32(3), 1159–1166. <https://doi.org/10.1016/j.matdes.2010.10.028>
- Basak, C.B., & Hari Babu, N. (2016). Morphological changes and segregation of β -Al₉Fe₂Si₂ phase: a perspective from better recyclability of cast Al-Si alloys. *Mater. Des*, 108, 277–288. <https://doi.org/10.1016/j.matdes.2016.06.096>
- Belov, N.A., Alabin, A.N., & Eskin, D.G. (2004). Improving the properties of cold rolled Al-6%Ni sheets by alloying and heat treatment. *Scripta Mater*, 50(1), 89–94. <https://doi.org/10.1016/j.scriptamat.2003.09.033>
- Belov, N.A., Eskin, D.G., & Aksenov, A.A. (2005). Multicomponent phase diagrams: applications for commercial aluminium alloys. Oxford: Elsevier.
- Belov, N.A., Alabin, A.N., Eskin, D.G., Istomin-Kastrovskiy, V.V. (2006). Optimization of hardening of Al-Zr-Sc casting alloys. *Journal of Material Science*, 41(18), 5890–5899. <https://doi.org/10.1007/s10853-006-0265-7>
- Belov, N.A., Naumova, E.A., Alabin, A.N., & Matveeva, I.A. (2015). Effect of scandium on structure and hardening of Al-Ca eutectic alloys. *Journal of Alloys and Compounds*, 646, 741–747. <https://doi.org/10.1016/j.jallcom.2015.05.155>
- Belov, N.A., Naumova, E.A., Akopyan, T.K., Doroshenko, V.V. (2017). Aluminium casting alloys on the base of ternary eutectic containing calcium and iron. In Z. Fan (Ed.), *Proceedings of the 6th decennial international conference on solidification processing*, BCAST, London (pp. 418–421).

- Booth-Morrison, C., Mao, Z., Diaz, M., Dunand, D.C., Wolverton, C., & Seidman, D.N. (2012). Role of silicon in accelerating the nucleation of Al₃(Sc,Zr) precipitates in dilute Al–Sc–Zr alloys. *Acta Mater*, 60(12), 4740–4752. <https://doi.org/10.1016/j.actamat.2012.05.036>
- Fuller, C.B., & Seidman, D.N. (2005). Temporal evolution of the nanostructure of Al(Sc,Zr) alloys: Part II-coarsening of Al₃(Sc_{1-x}Zr_x) precipitates. *Acta Mater*, 53(20), 5415–5428. <https://doi.org/10.1016/j.actamat.2005.08.015>
- Ji, S., Yang, W., Gao, F., Watson, D., & Fan, Z. (2013). Effect of iron on the microstructure and mechanical property of Al–Mg–Si–Mn and Al–Mg–Si die cast alloys. *Materials Science & Engineering*, 564, 130–139. <https://doi.org/10.1016/j.msea.2012.11.095>.
- Kaufman, J.G., & Rooy, E.L. (2004). Aluminum alloy castings: properties, processes, and applications. *ASM International*, Ohio.
- Kevorkov, D., & Schmid-Fetzer, R. (2001). The Al–Ca system, part 1: experimental investigation of phase equilibria and crystal structures. *Z Metallkd*, 92, 946–952.
- Knipling, K.E., Karnesky, R.A., Lee, C.P., Dunand, D.C., & Seidman, D.N. (2010). Precipitation evolution in Al–0.1Sc, Al–0.1Zr and Al–0.1Sc–0.1Zr (at.%) alloys during isochronal ageing. *Acta Materialia*, 58(15), 5184–5195. <https://doi.org/10.1016/j.actamat.2010.05.054>.
- Lefebvre, W., Danoix, F., Hallem, H., Forbord, B., Bostel, A., & Marthinsen, K. (2009). Precipitation kinetic of Al₃(Sc,Zr) dispersoids in aluminium. *J. Alloys Compd*, 470(1–2), 107–110. <https://doi.org/10.1016/j.jallcom.2008.02.043>.
- Liao, Hengcheng, Wu, Yuna, & Ding, Ke. (2013). Hardening response and precipitation behavior of Al–7%Si–0.3%Mg alloy in a pre-aging process. *Materials Science&Engineering*, 560, 811–816. <https://doi.org/10.1016/j.msea.2012.10.041>.
- Mondolfo, L.F. (1976). Aluminium alloys: structure and properties. Butterworths, London.
- Moustafa, M.A. (2009). Effect of iron content on the formation of β-Al₃FeSi and porosity in Al–Si eutectic alloys. *Journal of materials processing technology*, 209(1), 605–610. <https://doi.org/10.1016/j.jmatprotec.2008.02.073>.
- Reference data for thermodynamic calculations. <http://www.thermocalc.com>, 2017 (accessed 31.08.17).
- Røyset, J., & Ryum, N. (2005). Scandium in aluminium alloys. *International Materials Reviews*, 50(1), 19–44. <https://doi.org/10.1179/174328005X14311>
- Toropova, L.S., Eskin, D.G., Kharakterov, M.L., & Dobatkina, T.V. (1998). Advanced Aluminium Alloys Containing Scandium: Structure and Properties. Amsterdam: Gordon and Breach Science Publishers (pp. 175).
- Vlach, M., Stulikova, I., Smola, B., Piesova, J., Cisarova, H., Danis, S., Plasek, J., Gemma, R., Tanprayoon, D., & Neuber, V. (2012). Effect of cold rolling on precipitation processes in Al–Mn–Sc–Zr alloy. *Mat. Sci. Eng*, 548, 27–32. <https://doi.org/10.1016/j.msea.2012.03.063>.
- Zolotarevskiy, V.S., Belov, N.A., & Glazoff, M.V. (2007). Casting aluminum alloys. *Elsevier*, Amsterdam.